Geol. Soc. Malaysia, Bulletin 17, December 1984; pp. 357–371.

Analysis of Mesoscopic Structures at Mersing and Tanjung Kempit, Johore, Peninsular Malaysia

K.R. CHAKRABORTY and IAN METCALFE*
Department of Geology, University of Malaya, Kuala Lumpur, Malaysia.

Abstract: The metasedimentary rocks of possible Upper Palaeozoic age at Mersing and Tg. Kempit are multiply deformed. Using overprinting criteria as well as fold style and orientation, three phases of folding have been recognized, the second phase folds (F_2) being predominant. The structural evolutionary sequence in both the areas is similar, the first phase folds (F_1) are coaxially refolded by F_2, and F_3 folds are later superposed on both F_1 and F_2. Macroscopically, F_1 and F_2 folds are nonplane noncylindrical and F_3 folds appear to be plane noncylindrical.

The structural trends of the two areas are at variance. At Mersing, the F_1 and F_2 axial planes strike mainly northwesterly and axial plunge is towards southeast or northwest, while the trends of the F_1 and F_2 axial planes and axial plunge at Tg. Kempit are N to NNE.

F_1 and F_2 axes at Mersing are dispersed. The dispersion pattern may be interpreted as due to the superposition of F_3 folds of slip-type, the slip plane being subvertical and E-W trending with subhorizontal westerly a_3 kinematic axis. Alternatively, bending of the crustal block on a subvertical axis may be responsible for the dispersion of F_1 and F_2 as well as the development of F_3 folds. The difference in structural orientation between Mersing and Tg. Kempit is also explicable in terms of crustal bending. The postulated crustal bending may be envisaged as due to strike-slip motions.

INTRODUCTION

The metasedimentary rocks of probable Upper Palaeozoic age occuring along the length of the eastern coastal belt of Peninsular Malaysia show evidence for a polyphase sequence of deformational events, but the form, geometry and kinematics of the structures are not yet adequately known. A proper understanding of the structural evolution, including correlation of the structural sequence of the northern and southern sectors, of this deformed belt is essential for palaeotectonic reconstruction of the region. Over the last decade, structures of these deformed rocks have been studied by several workers (see, for example, Tjia, 1978a, 1978b, 1983; Yap and Tan, 1980 and the references therein), but these studies are mainly confined to the northern sector (Pahang and Trengganu). Very little published structural work is available from the southern sector (Johore). Recently the authors have made some structural studies at two localities, Mersing and Tanjung Kempit, in the southern sector (see Fig. 1 for location). Coastal outcrops of deformed metasediments (mainly quartzite and slate/phyllite) at these two areas exhibit many interesting structural features. In this paper the results of a preliminary analysis of the mesoscopic structures observed at these two localities are presented. The general geological accounts of these two areas are given by Mah (1972), Lee (1972) and Roslant (1981).

Using overprinting criteria (Hopgood, 1980; Hobbs et al., 1976) as well as deformational style and orientation, the effects of three phases of deformation have

*Present address: 6E, Lorong 16/10C, Petaling Jaya, Selangor, Malaysia.

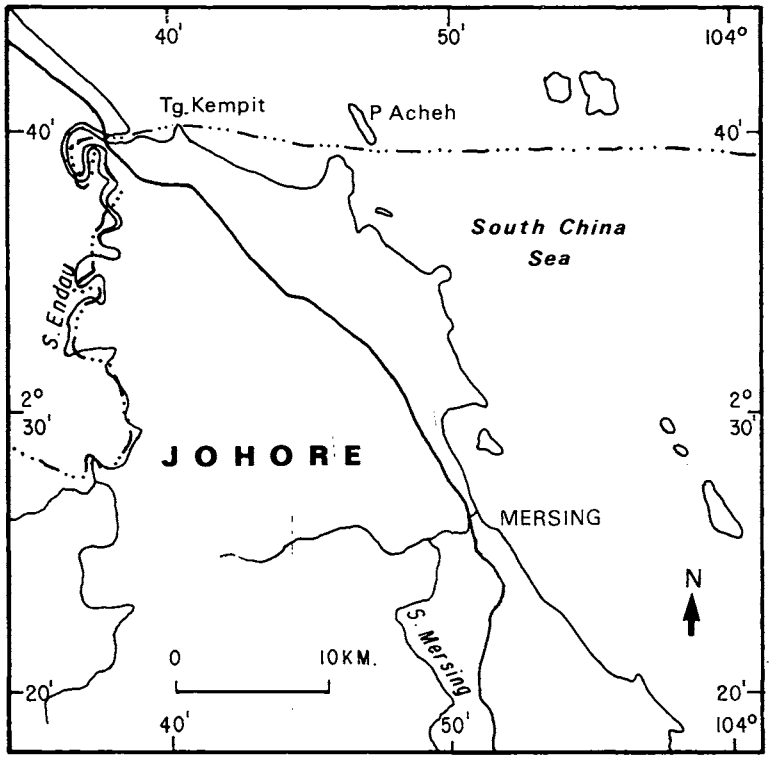

Fig. 1 Location map.

been recognized in both the areas (Figs. 2 and 6). For brevity and convenience the structural elements corresponding to the three phases will be denoted by the following abbreviations:

D_1, D_2, D_3 = First, second and third deformational phases respectively.

F_1, F_2, F_3 = Folds of the first, second and third phases respectively.

S_0 = Bedding surface

S_1, S_2, S_3 = Axial planes of F_1, F_2 and F_3 respectively and the surfaces parallel to them.

a, b, c = Kinematic axes of folding, with subscript denoting the phase of folding.

MERSING

Structural studies at Mersing have been confined to the good coastal outcrops along a stretch of about 3 km from the Rest House to the airport. The rocks are highly

Fig. 2. Mesoscopic folds at Mersing.

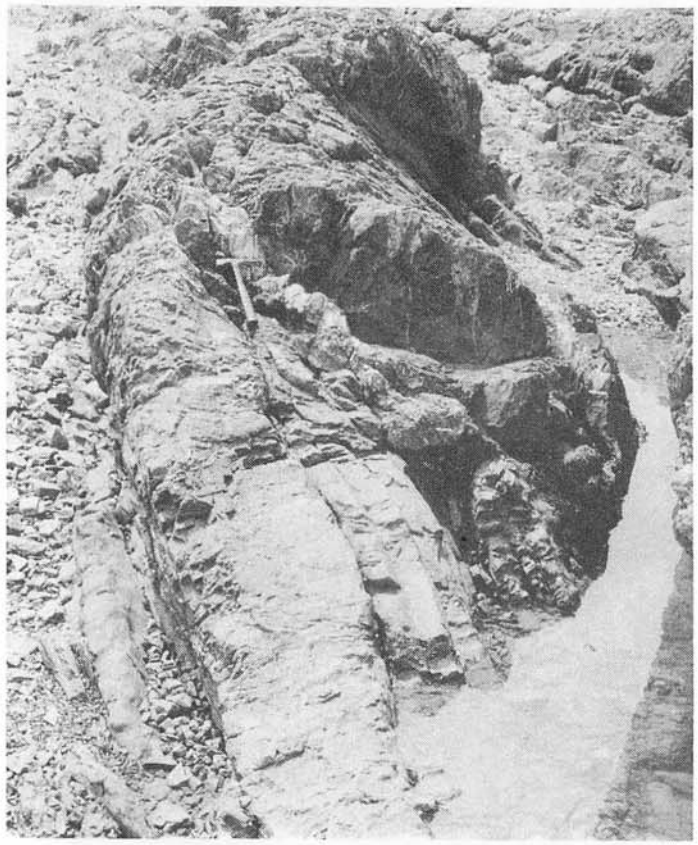

Fig. 2(a). Isoclinal F_1 fold with overprint of F_2 fold noticeable in the right hand side limb. The whole fold is bent due to D_3. Note the thick quartz vein (near the hammer) parallel to the F_1 axial plane, and finer quartz veins parallel to the F_2 axial plane. View towards SE.

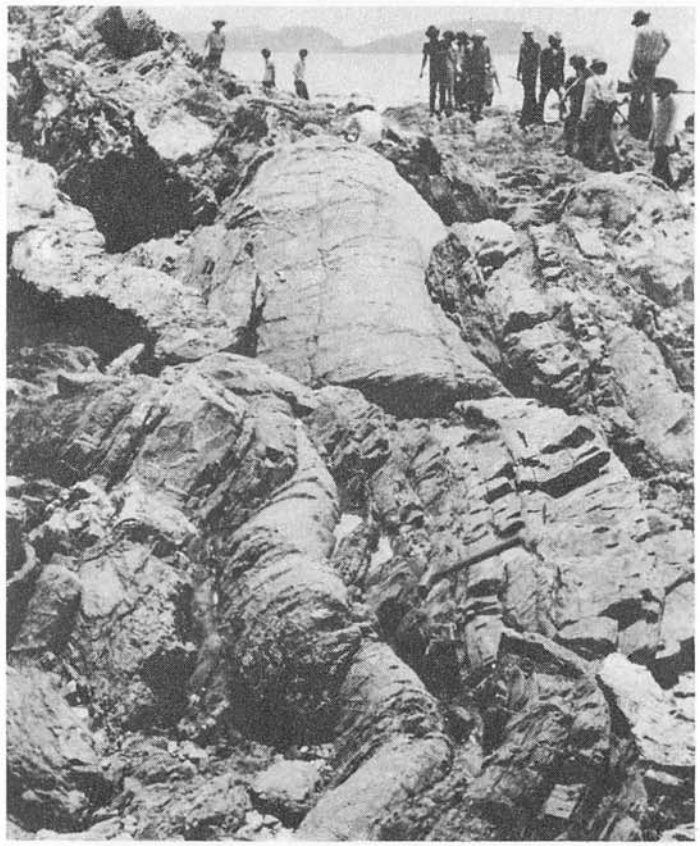

Fig. 2(b). F_1 hinge folded by F_3. View towards NNE.

Fig. 2(c). Tightly appressed F_2 fold with gently curved steeply dipping axial plane. Note the small isoclinal (reclined) F_1 fold in the right hand limb of F_2 near the lower right hand corner. The pole is about 2m. View towards SE.

Fig. 2(d). Symmetrical F_2 folds. Note the bending of the hinge line and axial plane due to D_3 deformation. View towards S.

Fig. 2(e). Isoclinal synformal F_2 fold. Note the rounded hinge. View towards S.

deformed and folded (Fig. 2), but bedding is well preserved. The beds are frequently overturned as evident from the geometry of fine scale cross bedding, graded bedding and bedding–cleavage relationship or from the exposures of overturned folds. The beds show variable attitudes because of multiple deformation, but in general they have a northwesterly strike. The dip is predominantly southwesterly as the southwesterly dipping limbs of the folds are usually longer and better developed. The northeasterly dipping limbs of asymmetric folds are generally steeper. Axial planar foliation has developed in slates and phyllites, and is commonly parallel to, or makes a small angle with, the bedding except in the hinge areas of the folds. Linear structures are not very well developed, but puckering on foliation, bedding-cleavage intersection, quartz rods, mullions and boudins can be seen in places. Folded as well as pinch-and-swell structured quartz veins are quite frequent. Faults, both parallel and transverse to the axial plane trends, are common; however, they have not been included in the present study. There are some isolated narrow elongated elliptical structures closed at both ends. These structures are restricted in quartzite lithology. It is not clear whether they are very tight fold closures or drawn out boudins. Measurements from these structures are omitted from the structural analysis.

First Phase Folds (F_1)

The F_1 folds are tight and isoclinal (sometimes reclined) to overturned (Fig. 2) with

axial planes commonly dipping southwesterly. The attitude of the axial plane (S_1), however, varies due to the effects of the later phase deformations. In many isolated cases F_1 folds are seen to be overprinted by F_2 and F_3 (Fig. 2). F_1 generally plunges southeasterly at low to moderate angles, but northwesterly plunge is not uncommon. In places, the reversal of plunge direction can be traced through a subhorizontal stage. Macroscopic F_1 folds are thus nonplane noncylindrical.

Axial planar foliation (S_1) defined by phyllosilicates can be seen in pelitic/semipelitic units. In more competent quartzites S_1 is expressed by fracture cleavage commonly filled with quartz. Folded S_1 can be seen in F_2 hinges, and this is particularly noticeable in thin sections of F_2 profiles. S_1 may be puckered, and $S_0 \times S_1$ intersection lineation can occasionally be seen.

Second Phase Folds (F_2)

Folds of the second phase are most abundant in the area. The size and style of F_2 folds are variable. They are mostly asymmetrical, but overturned and isoclinal folds are not uncommon. Symmetrical upright folds of this phase may also be encountered (Fig. 2). Variations in style along axial traces can occasionally be seen. The folds are usually tight, but may be open and fold apices may be sharp or round. The F_2 folds and their axial planes (S_2) have been deformed by D_3 resulting in arcuate or sinuous outcrop patterns of many F_2 folds. The angle and direction (including reversal) of plunge of F_2 folds are similar to those of F_1 and therefore they are likely to be coaxial. Like F_1, macroscopic F_2 folds are also nonplane noncylindrical.

In absence of overprinting features, overturned and isoclinal F_2 folds and corresponding S_2 cannot readily be separated from F_1 and S_1 on the basis of style and orientation. It is possible that isolated overturned or isoclinal folds identified as F_2 may, in fact, be F_1 and vice versa. More detailed work would be necessary to overcome this difficulty and to establish more reliably the true geometric relationship between F_1 and F_2.

Axial planar foliation, occasionally puckered, is visibly developed in pelites and the $S_0 \times S_2$ intersection lineation can be seen in places. Boudins of more competent layers occur on the limbs of F_2 (and F_1?) folds. Structural discontinuites with detachment of limbs from nose are quite frequent due to axial planar movement.

Third Phase Folds (F_3)

Folds of the third phase, though common, are weakly expressed. They are asymmetrical to symmetrical open folds with low amplitude/wavelength ratio. Axial planes are steeply dipping to subvertical with broadly easterly strike. The orientation and plunge of the individual F_3 folds vary depending upon the preexisting structure and the position of their development on the limbs of the earlier folds. Individual F_3 folds die out along their axial surface trends.

Structural Analysis

The Mersing area is heterogenous with respect to bedding (S_0) which is the most dominant planar structure. In Figs. 3a and b, equal area projections of 320 bedding

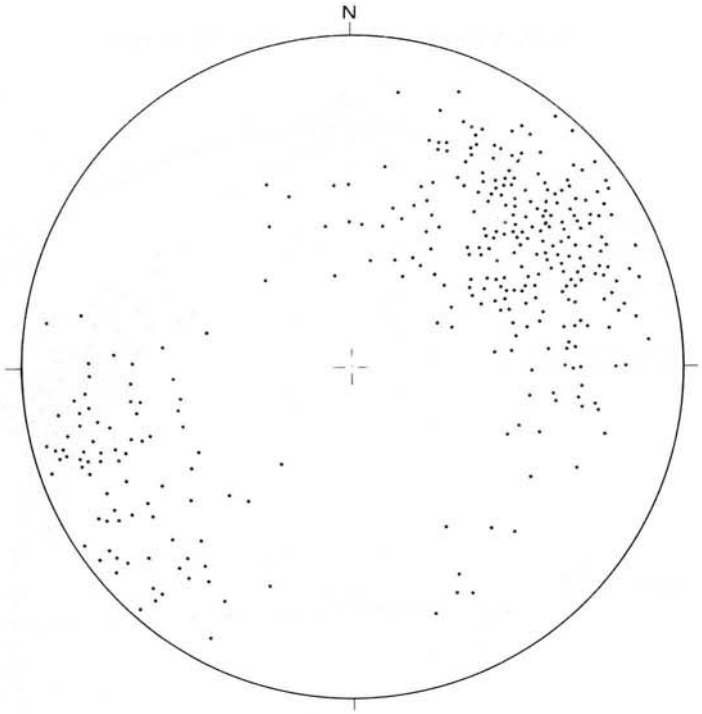

Fig. 3(a). Lower hemisphere equal area projections of 320 bedding poles from Mersing.

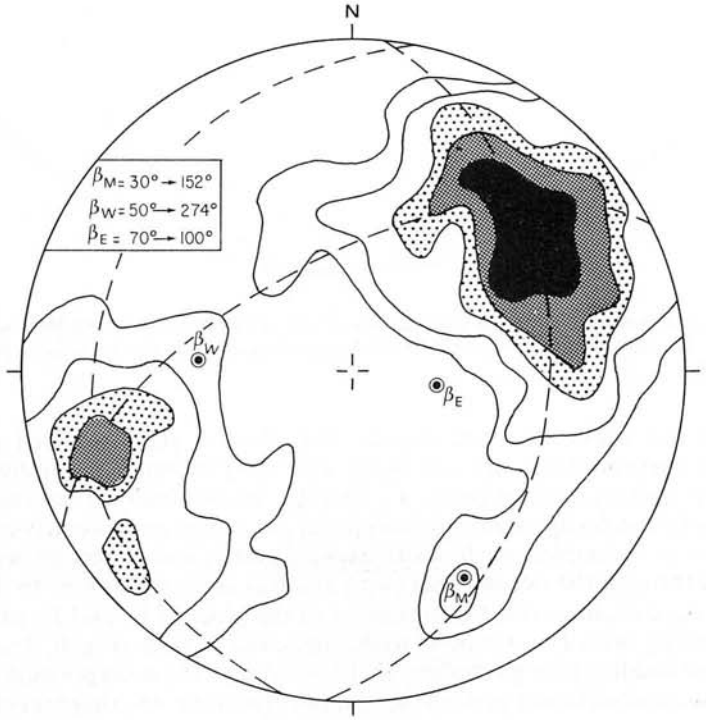

Fig. 3(b). Contoured diagram of bedding poles showing three girdles (see text). Contours at 0.3, 1, 2, 3 and 6% per 1% area.

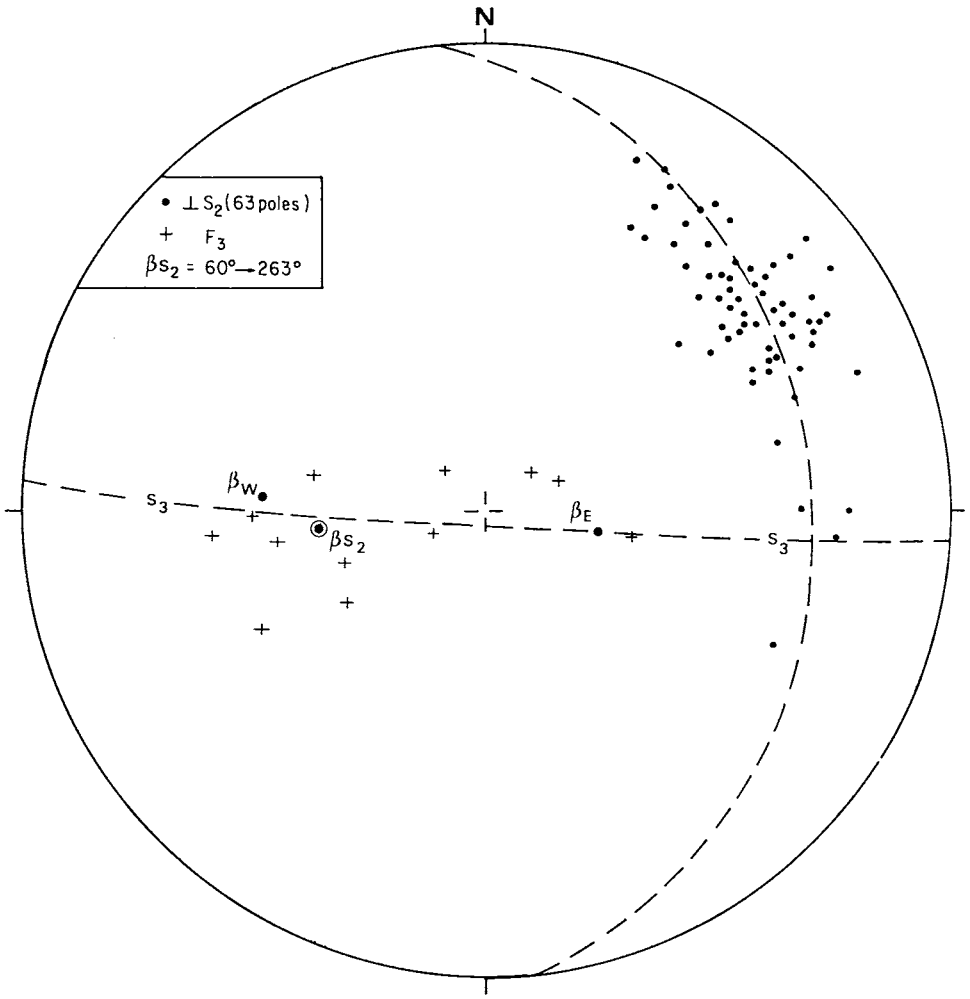

Fig. 4 Lower hemisphere equal area projections of S_2 (F_2 axial plane) poles from Mersing. βS_2 is the axis of the π-circle. Measured F_3 fold axes are also plotted. β_E and β_W are from Fig. 3b. S_3 is the plane defined by β_E, β_W and βS_2.

poles from the whole area are shown. The plots display two well defined but unbalanced maxima which are consistent with the predominant southwesterly and subordinate northeasterly dipping F_1 and F_2 limbs observed in the field. The distributin of the poles apparently define partial great circle girdles of a compound type where a pair of incomplete girdles with axes β_W and β_E can be recognized across the main girdle through the two maxima (with axis β_M) as shown in Fig. 3b. It should be noted that β_M coincides with the maximum of the plots of F_1 and F_2 axes (Fig. 5b) while β_W and β_E broadly correspond to the measured F_3 folds (Fig 4). The compound nature of the bedding pole girdles are, therefore, due to the superposition of F_3 on F_1 and F_2. This interpretation gets further support from the πS_2 diagram (Fig. 4). The

plots of S_2 poles are spread along a partial great circle indicating cylindrical folding of S_2 by D_3. It may be noted that βS_2 broadly agrees with β_W (Fig. 4). Since, as pointed out earlier, S_2 is subparallel to the southwesterly dipping limbs of the F_2 folds, the coincidence of βS_2 and β_W suggests that the southwesterly limbs of the earlier folds have been similarly folded by D_3. The partial girdle with axis β_E, by implication, is the consequence of folding of the northeasterly dipping limbs of the earlier folds. The limbs of the earlier folds thus appear to have responded to D_3 by folding about different axes, β_E and β_W, because of the difference in their attitude. It is implicit that β_E, β_W and βS_2 would share a common axial plane which is also the regional F_3 axial plane. The plane passing through them thus defines the F_3 axial plane (S_3) as shown in Fig. 4. Note that the individual F_3 folds also, by and large, lie along this plane (Fig. 4). The cylindrical folding of S_2, as indicated by the S_2 pole diagram (Fig. 4), is an evidence for an initial (pre-F_3) plane form of the F_2 folds implying that the present nonplane form of F_2 is due to D_3 deformation. The F_3 folds, characterized by variously oriented axes but broadly constant axial plane orientation, are plane noncylindrical.

The axes of F_1 and F_2 folds and related b-lineations (puckering, bedding-cleavage intersection) are plotted in Fig. 5. F_1 and F_2 are treated together because of the difficulties of sure recognition as pointed out earlier. It is apparent from Fig. 5 that F_1 and F_2 do not maintain constant orientation, they are distinctly dispersed evidently because of the effect of D_3 deformation. In superposed fold systems, the manner in which the earlier folds are deformed depends on the mechanism of the later folding (see, for example, Turner and Weiss, 1963; Ramsay, 1967). The earlier fold axes (mesoscopic) may be dispersed along a small circle centred on the later fold axis (if the fold axis is the kinematic b-axis, e.g. flexural slip fold) or along a great circle oblique to the later fold axis (fold axis is not the b-kinematic axis, e.g. common slip folds).

The F_1 and F_2 axes are dispersed in such a manner that both a small circle and a great cirlce can describe the pattern equally well (Fig. 5b) and therefore amenable to alternative interpretations. The best-fit small circle is centred on a vertical axis which does not coincide with β_E, β_W or βS_2 (hence F_3 axis is not the b_3 kinematic axis). The dispersion of the F_1 and F_2 axes is clearly not due to rotation about F_3 axis but may be a result of crustal bending on a subvertical axis. On the other hand, if the great circle dispersion is taken, then it would imply that F_3 folds are slip folds and that the geometrically constructed F_3 axial plane (S_3) is the slip plane containing the a_3 and b_3 kinematic axes. Since a_3 must also lie on the F_1 and F_2 great circle, its intersection with S_3 defines the a_3 kinematic axis of F_3 folding (Fig. 5b). The other kinematic axes can be easily located, b_3 lies 90° from a_3 along S_3, while c_3 is normal to a_3b_3 plane (i.e. S_3). It may be noted from Fig. 5b that a_3 is subhorizontal (gentle westerly plunge) and b_3 is subvertical, and accordingly the development of F_3 folds can be considered as due to subhorizontal slip (parallel to a_3). The two alternative interpretations based on the small circle and great circle pattern, are not mutually exclusive and can be accommodated within a single unifying model.

TANJUNG KEMPIT

Deformed metasediments, lithologically similar to those at Mersing, are exposed over a very small area around the tip of Tg. Kempit. The structure of this area has been briefly described by Tjia (1978b).

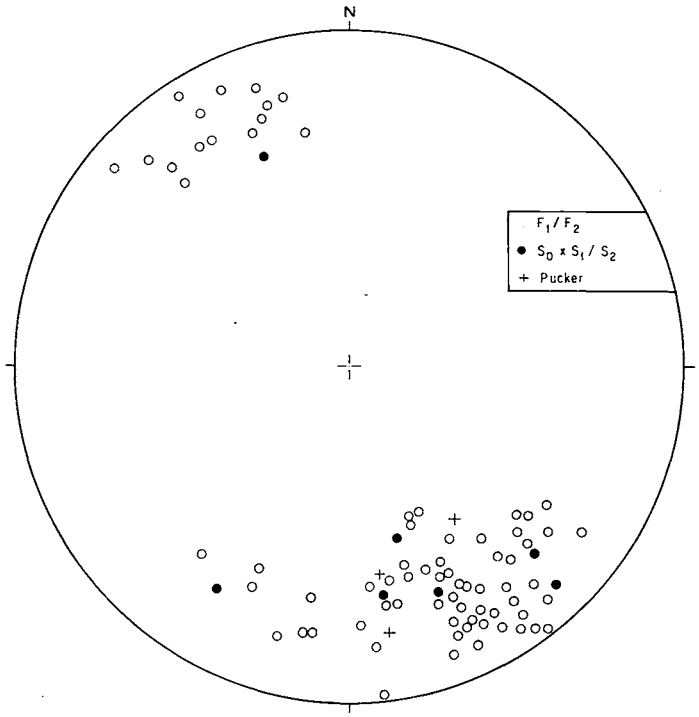

Fig. 5(a). Lower hemisphere equal area projections of F_1 and F_2 axes and related lineations from Mersing (83 plots).

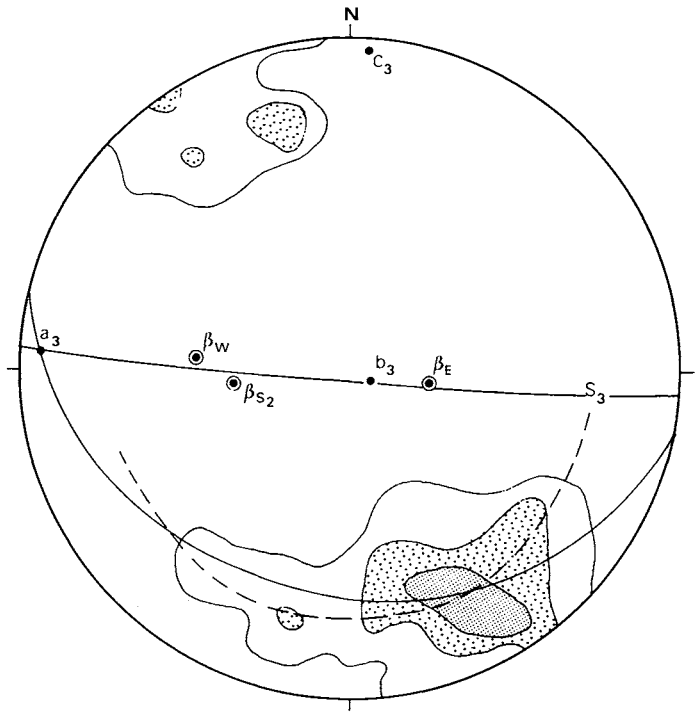

Fig. 5(b). Contoured diagram of (a). Contour intervals at 1, 5 and 10 % per 1 % area. A small circle (broken line) and a great circle (full line) are fitted through the girdle. The small circle is centred on a vertical axis. The plane S_3 is from Fig. 4. a_3, b_3 and c_3 are the inferred kinematic axes, a_3 and b_3 lie on S_3, and c_3 is normal to S_3. a_3 is the intersection of the great circle and S_3.

The F_1 folds are not common in Tg. Kempit, only a few definite F_1 folds, refolded by F_2, have been observed (Figs. 6–8). F_1 folds are isoclinal, and one example of an isoclinal reclined fold has been found where the strike of the axial plane is approximately normal to the trend of the fold axis. F_1 folds plunge moderately towards N to NNE (Fig. 9). The F_1 axial planes (S_1) vary in attitude as they are folded by F_2 (Figs. 6–8 and 9).

F_2 folds are the main structures observed at Tg. Kempit. The area is homogeneous with respect to F_2. These folds vary in style from highly appressed to relatively open with rounded to sharp hinges. The variation in hinge shape may sometimes be noticed in the different beds within a single fold. The F_2 axial planes (S_2) have a general N-S strike and steep dip easterly or westerly. F_2 fold axes do not show any significant variation in orientation and have moderate plunge towards N to NNE like F_1 folds. Convergent axial plane fractures, often filled with quartz, are very common and their intersection with the bedding forms the most conspicuous lineation (parallel to F_2) in the area.

F_3 folds are weakly expressed in Tg.Kempit area and occur as small warps in the limbs of the earlier folds. The F_3 axes are variably oriented usually with steep plunge.

Equal area projections of bedding poles, F_1 and F_2 axes and intersection lineations are shown in Fig. 9. The bedding poles are spread along a well defined great

Fig. 6. Reclined F_1 fold (closure near the left margin shown by the thick quartzite) coaxially refolded by F_2, View towards N.

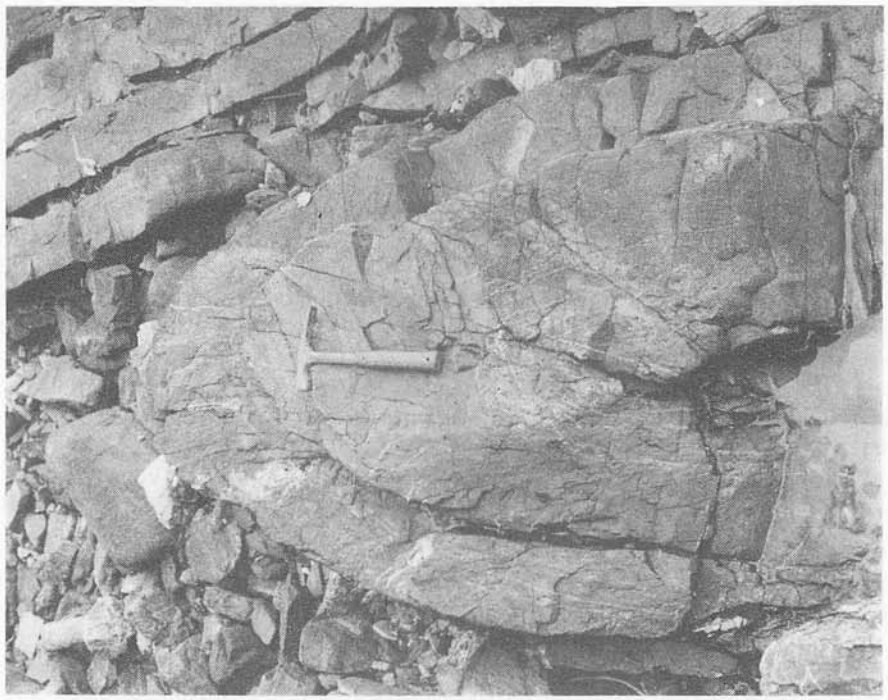

Fig. 8. Tight F_2 fold with subvertical axial plane. Note the folded thin quartz veins below the hammer handle. They represent the F_1 axial plane. Also note the convergent fractures filled with quartz.

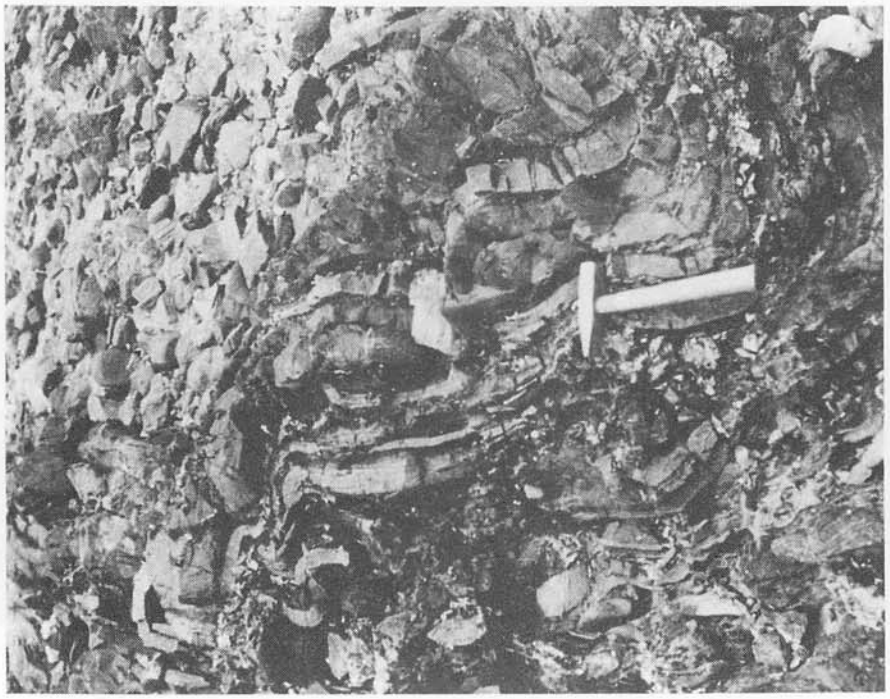

Fig. 7. Isoclinal F_1 refolded by F_2. F_2 hinge is near the hammer. F_1 closure can be seen at the top left corner. Warping of the limbs are F_3. View towards N.

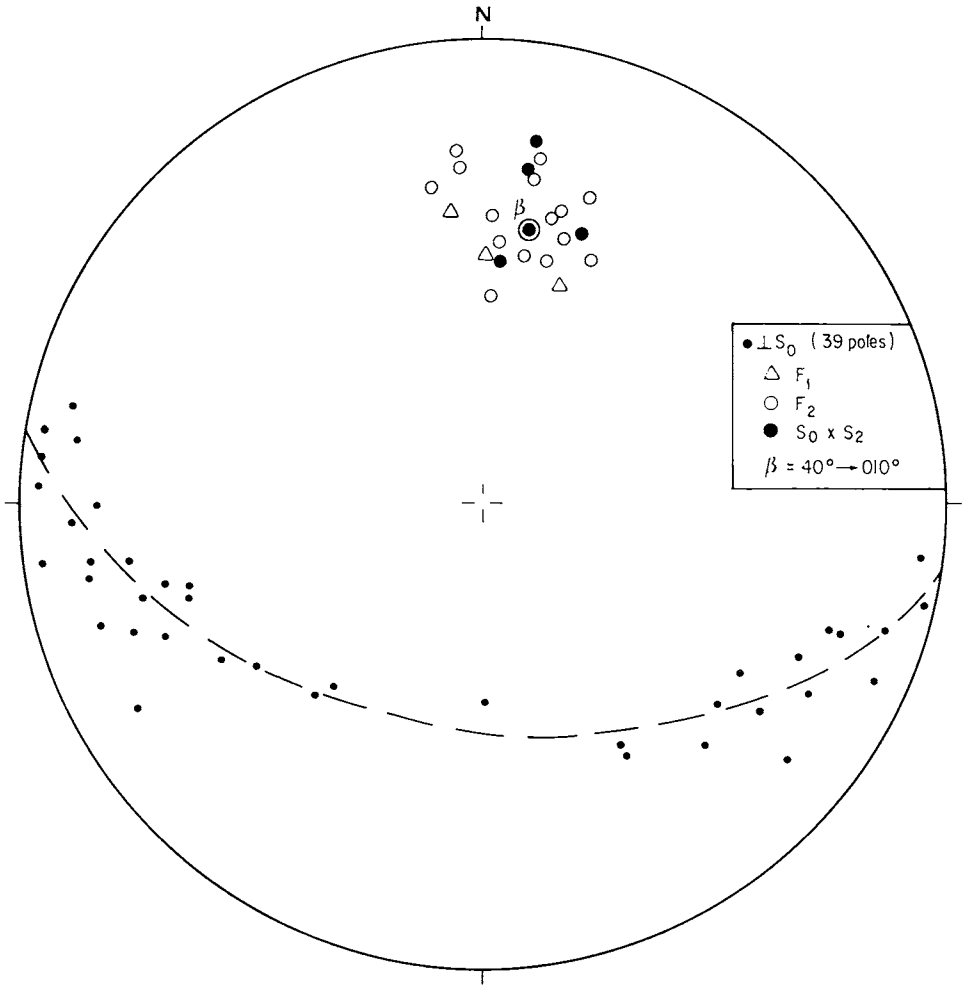

Fig. 9. Lower hemisphere equal area projections of bedding poles, F_1 and F_2 axes and $S_0 \times S_2$ lineations from Tg. Kempit. β is the axis of the π-circle.

circle with axis β (plunge 40° → 010°) which coincides with the measured F_2 fold axes and the $S_0 \times S_2$ lineations. The orientations of the F_2 axes and S_2 are more or less constant indicating that the F_2 folds at Tg. Kempit are plane cylindrical. It is of interest to note that the mean beta-intersection of S_1 and S_2 (Fig. 10) is identical to βS_0 (Fig. 9) indicating that S_0 and S_1 are cofolded about the same axis (= F_2). This implies that prior to F_2, S_0 and S_1 were mutually parallel confirming the isoclinal nature of the F_1 folds. The coincidence of F_1 and F_2 axes, βS_0 and $S_1 \times S_2$ suggests that isoclinal F_1 folds have been coaxially refolded by F_2 folds.

DISCUSSION

It is apparent from the above analysis that the structural evolution, both in nature

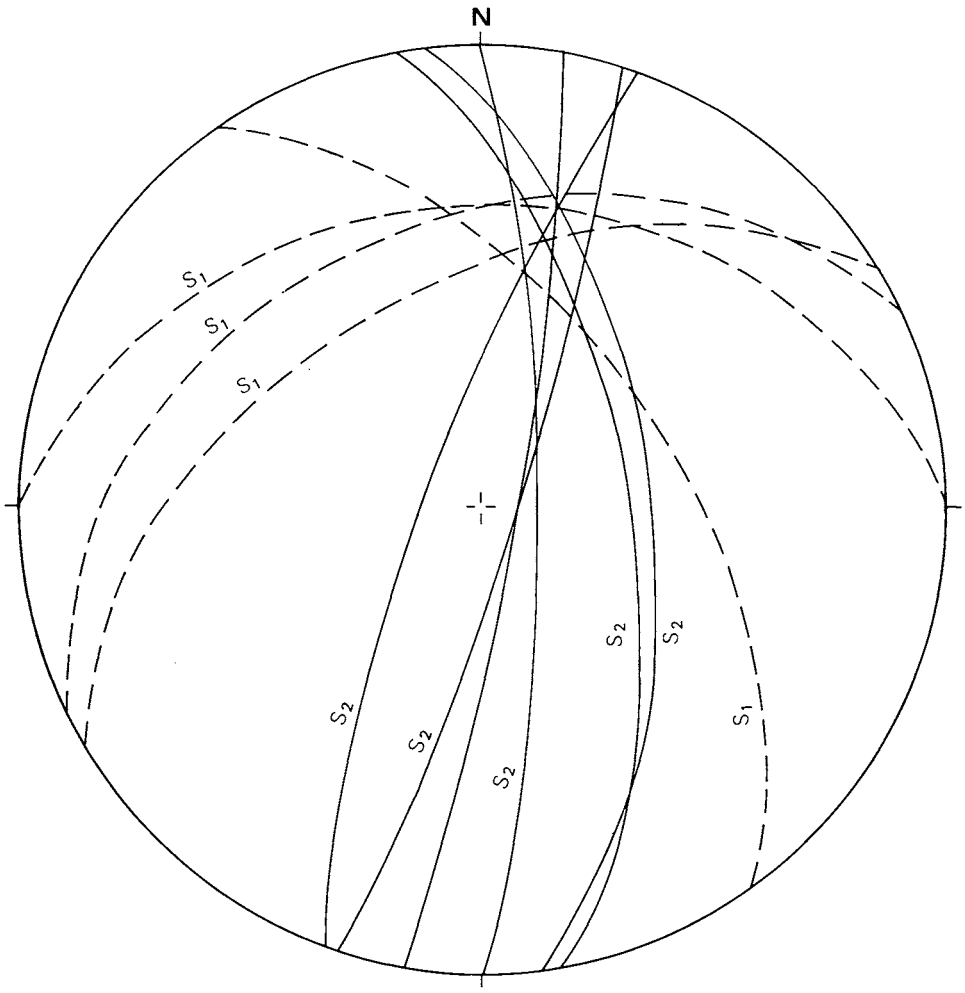

Fig. 10. Lower hemisphere equal area projections of F_1 axial planes (S_1) and F_2 axial planes (S_2) from Tg. Kempit.

and sequence, of the two areas is essentially similar. The conspicuous difference, however, is the orientation of the F_1 and F_2 folds. While the axial surface trend at Mersing is mainly NW-SE and axial plunge towards SE or NW, those at Tg. Kempit are mainly N to NNE. If the unlikely possibility that the folds in the two areas have formed at different times under different stress systems is excluded, then the difference in structural orientation can be explained by (i) local variation in the stress orientation during D_1 and D_2 deformation, or (ii) later rotation (but not about F_3 axis) during D_3 deformation. It may be of significance in this context to note that the northwesterly plunging F_1 and F_2 axes of Mersing can be brought into coincidence with those of Tg. Kempit by rotation on a subvertical axis which corresponds closely to the axis of rotation inferred from the small circle dispersion pattern of F_1 and F_2 at Mersing. Thus

the difference in structural orientation between the two areas caused by rotation due to bending of crustal block seems a distinct possibility. A likely cause for such block bending may be strike-slip motion. A somewhat similar case of structural rotation in the East Fork area of the San Gabriel Mountains has recently been discussed by Jacobson (1983) who attributes the rotation to bending caused by movements on the San Andreas and Punchbowl faults.

An important question that needs attention is whether the three folding phases are widely separated in time—a problem endemic to all multiply deformed belts. Coaxially refolded folds are easily generated through continuous deformation, and hence F_1 and F_2 folds of the two areas may be cogenetic representing successive stages of a single deformational event. The contrasting geometric pattern and inferred kinematics of F_3 folds may suggest a different event separated in time.

The deformed metasediments are overlain by essentially undeformed acidic extrusives of probable Triassic age (Mah, 1972). The F_1 and F_2 folding may, therefore, be regarded as a Permo-Triassic event. The timing of F_3, however, cannot be constrained and remains open to speculation.

ACKNOWLEDGEMENT

This study was supported by the University of Malaya Research Grants Nos. F28/78 (KRC) and F142/77 (IM). The diagrams were prepared by the Drafting Section of the Department of Geology, University of Malaya.

REFERENCES

HOBBS, B.E., MEANS, W.D. and WILLIAMS, P.F. (1976). An Outline of Structural Geology. John Wiley, New York.

HOPGOOD, A.M. (1980). Polyphase fold analysis of gneisses and migmatites. Trans. R. Soc. Edinburgh Earth Sci., 71, 55-68.

JACOBSON, C.E. (1983). Structural geology of the Pelona Schist and Vincent thrust, San Gabriel Mountains, California. Bull. Geol. Soc. Am., 94, 753-767.

LEE, S.C. (1972). The geology of the Mersing area. Unpubl. B.Sc. (Hons) thesis, Dept. of Geology, Univ. of Malaya.

MAH, W.H. (1972). The geology of the area southeast of Endau, Johore, Malaysia. Unpubl. B.Sc. (Hons) thesis, Dept. of Geology, Univ. of Malaya.

RAMSAY, J.G. (1967). Folding and Fracturing of Rocks. McGraw-Hill, New York.

ROSLANT BIN ABU (1981). Stratigraphy and petrography of the Mersing area, Johore. Unpubl. B.Sc. (Hons) thesis, Dept. of Geology, Univ. of Malaya.

TJIA, H.D. (1978a). Multiple deformation at Bukit Cenering, Trengganu. Bull. Geol. Soc. Malaysia, 10, 15-24.

_____ (1978b). Structural geology of Peninsular Malaysia. Proc. GEOSEA III, Bangkok (ed. P. Nutalaya), 673-682.

_____ (1983). Canggan bertindan di Tanjung Gelang, Pahang. Sains Malaysiana, 12, 101-117.

TURNER, F.J. and WEISS, L.E. (1963). Structural Analysis of Metamorphic Tectonites. McGraw-Hill, New York.

YAP, L.S. and TAN, B.K. (1980). Deformation of the Upper Palaeozoic rocks at Tanjung Gelang, Pahang. Bull. Geol. Soc. Malaysia, 12, 45-54.

(Manuscript received on 8th Dec. 1984)